Temperature and density dependence of the self-diffusion coefficient and Mori coefficients of Lennard-Jones fluids by molecular dynamics simulation

María J. Nuevo and Juan J. Morales
Departamento de Física, Facultad de Ciencias, Universidad de Extremadura, 06071 Badajoz, Spain

David M. Heyes
Department of Chemistry, University of Surrey, Guildford GU2 5XH, United Kingdom
(Received 23 October 1996)

The ability of a Mori series expansion to predict the self-diffusion coefficients of Lennard-Jones (LJ) fluids has been tested for a wide range of temperatures ($4.45 \geqslant T^* = kT/\epsilon \geqslant 0.71$) and densities ($1.04 \geqslant \rho^* = \rho\sigma^3/\epsilon \geqslant 0.20$). The self-diffusion coefficients and the Mori series coefficients were calculated from the same molecular dynamics simulations and fitted to simple analytic expressions. Exponential, Gaussian, secant hyperbolic, and Joslin-Gray memory functions up to the first two Mori coefficients have been used in the analytic expressions for the self-diffusion coefficient. The Mori coefficients exhibit a near linear dependence with temperature in the stable fluid phase, with the second Mori coefficient being strongly temperature but more weakly density dependent (confirming earlier simulation results of Lee and Chung). On balance it appears that the Gaussian memory function gives the best agreement with the simulation diffusion coefficients considering the whole LJ phase diagram. Also we find that at low densities the Gaussian approximation for the diffusion coefficient follows the expected $\sqrt{T^*}/\rho^*$ limiting behavior. [S1063-651X(97)04304-3]

PACS number(s): 66.10.−x, 82.20.Tr, 82.20.Wt

I. INTRODUCTION

Transport coefficients calculated using the Green-Kubo (GK) integral formulas require appropriate correlation functions which can, in principle, be calculated by molecular dynamics (MD) computer simulation. The self-diffusion coefficient D or shear viscosity η for example, require the velocity or the off-diagonal pressure tensor component autocorrelation functions in the (GK) integrand. Approximate expressions for the transport coefficients can be written using the generalized Langevin equation (GLE) formulation for the time correlation function in terms of a hierarchy of memory functions. The problem that arises is that the analytic form of the memory function has to be proposed. In general, the memory function $M(t)$ belongs to a set of functions $M_n(t)$, with $n=0,1,2,\ldots$, which obey the set of coupled Volterra equations [1]. The Laplace transform $\tilde{M}(s)$ first derived by Mori [2] can be written as a infinite continued fraction including the so-called *damping matrices* or *Mori coefficients* K_n and are the zero-time values of the memory function $M_n(0+)$. Thus, the predicted value for a given transport coefficient will be affected by the manner in which the Mori series is truncated [3]. A variety of closure schemes and analytic forms for the memory function have been proposed that give reasonable predictions for the transport coefficients going up to the sixth frequency moment of the time correlation function [4,5]. The second frequency moment is associated with the first Mori coefficient K_1, the fourth frequency moment with the second Mori coefficient K_2, and so on [4].

The overall conclusion from these studies is that the first two Mori coefficients give reasonable values for the transport coefficients. Also there is no apparent advantage in going to higher-order terms as these Mori coefficients are difficult to compute with any precision. This is a problem as the series does not appear to be rapidly convergent. The accuracy of evaluation of the Mori coefficients deteriorates rapidly with increasing n and also becomes progressively more sensitive to the procedure used to evaluate the moments [3,5]. The most important factor influencing the agreement with exact (i.e., simulation) values appears to be the analytic form chosen for the memory function, which is still arbitrary and not surprisingly the optimum form varies with the state point.

The use of only the first two Mori coefficients means that a short-time memory function is implicitly being considered in the self-diffusion coefficient study. Even though it is known that the self-diffusion coefficient also depends on the medium- and long-time memory function, as was discovered by Levesque and Verlet [6], and systematically tested in a later extensive molecular dynamics investigation of the bimodal relaxations time models for the memory function by Lee and Chung [7]. Its dependence on the intermolecular potential has also been investigated [3]. It is nevertheless evident that in a number of recent simulation studies (e.g., based around information theory [4,5]) that the transport coefficients of the Lennard-Jones fluids are reasonably well accounted for by the two first Mori coefficients. All practical applications of Mori theory for the memory function are limited to relatively low-order expansions. Therefore, we focus our study on the state point dependence of the first two Mori coefficients in order to make progress in choice of closure and to compare our results with the previous works at the same state points. The inclusion of the medium and long relaxation times require higher-order Mori coefficients to be included in the Mori expansion [7] for the self-diffusion coefficient. It could be argued that the discovery of an optimum

analytic form for the memory function at the K_1 and K_2 level will incorporate these long-time effects semiempirically by virtue of a mean-field cancellation of errors.

Before further progress can be made it is useful to discover how the lower Mori coefficients depend on temperature and density, which might lead to improved closure procedures. In this paper we investigate further the dependence of the self-diffusion coefficient D on temperature T and density ρ, and the relative merits of the closure schemes in the Mori series as a function of the state point. In order to make progress in choice of closure we focus on the state point dependence of the first two Mori coefficients. Our results will be compared with the previous works at the same state points [8,4,9]. In Sec. II will be described the theoretical background needed to obtain the self-diffusion coefficient directly from the mean-square displacements by equilibrium MD and also in terms of the two first Mori coefficients using different mathematical solutions for the truncated Mori expansion. In Sec. III the simulation details are described, leading to Sec. IV with the results and the discussion and conclusions in Sec. V.

II. THEORETICAL BACKGROUND

The self-diffusion coefficient of particle i can be obtained directly from MD computer simulation from the linear region of the mean-square displacement (MSD) as [10]

$$D_i = \lim_{t\to\infty} \frac{\langle |\mathbf{r}_i(t)-\mathbf{r}_i(0)|^2\rangle}{6t}, \tag{1}$$

where $\mathbf{r}_i(t)$ is the absolute position of particle i at a time t after an arbitrarily defined time origin and $\langle\cdots\rangle$ denotes the time average.

Alternatively and according to the GLE formalism, the diffusion coefficient can be obtained by the evaluation of the time autocorrelation function of the velocity as

$$D = \frac{kT}{m}\int_0^\infty \frac{\langle v_\alpha(t)v_\alpha(0)\rangle}{\langle v_\alpha^2\rangle}\,dt = \frac{kT}{m\widetilde{M}(0)}, \tag{2}$$

where k is the Boltzmann constant, v_α is a Cartesian component of the velocity of an atom of mass m, and $\widetilde{M}(0)$ is the Laplace transformation of the memory function at zero frequency, values of which are expressed in terms of the Mori coefficients. For example, for the fourth frequency moment (up to the second Mori coefficient) we have the generic form

$$\widetilde{M}(0) = \int_0^\infty M(t)dt = \int_0^\infty K_1 f(K_2,t)dt. \tag{3}$$

The coefficients can be obtained from the time average of the nth time derivative of the normalized velocity as

$$U_n = \frac{1}{N}\left\langle \sum_{i=1}^{N} \mathbf{v}_i^n\cdot\mathbf{v}_i^n \right\rangle, \tag{4}$$

being the first two Mori coefficients calculated as [11]

$$K_1 = U_1 = \frac{m}{3NkT}\left\langle \sum_{i=1}^{N} \mathbf{a}_i^2 \right\rangle, \tag{5}$$

where $\mathbf{a}_i$ is the acceleration of particle i, and

$$K_2 = \frac{U_2}{K_1} - K_1. \tag{6}$$

An exact solution for the memory function in Eq. (2) is not known and therefore assumptions must be made about its analytic form. Several analytic memory-function closures are investigated here, employing up to the first two Mori coefficients. These are the exponential exp, Gaussian G, secant hyperbolic sech, and Joslin and Gray [12], (JG) closures as discussed in Ref. [4]. The first three closures use the named mathematical functions and the last closure is an alternative prescription based on the geometric mean of the two successive Mori coefficients. These memory functions are

$$M_{\rm exp}(t) = K_1 e^{-K_2^{1/2}t}, \tag{7}$$

$$M_G(t) = K_1 e^{-K_2 t^2/2}, \tag{8}$$

$$M_{\rm sech}(t) = K_1 \,{\rm sech}(-K_2^{1/2}t), \tag{9}$$

and

$$M_{\rm JG}(t) = K_1 e^{-(K_2K_1)^{1/4}t}, \tag{10}$$

which are used to calculate $\widetilde{M}(0)$ in Eq. (3), being the time integration of function $f(K_2,t)$. Substitution in Eq. (2) gives the corresponding self-diffusion coefficients,

$$D_{\rm exp} = \frac{kT}{m}\frac{K_2^{1/2}}{K_1}, \tag{11}$$

$$D_{\rm G} = \sqrt{2/\pi}D_{\rm exp}, \tag{12}$$

$$D_{\rm sech} = \frac{2}{\pi}D_{\rm exp}, \tag{13}$$

and

$$D_{\rm JG} = \left(\frac{K_1}{K_2}\right)^{1/4} D_{\rm exp}, \tag{14}$$

where all the diffusion coefficient closures have been expressed explicitly in terms of the exponential closure, with different multiplying constants in the case of the Gaussian and secant hyperbolic closures, and in terms of the K_1 and K_2 ratio for the Joslin-Gray closure. Note that the first three, Eqs. (11)–(13) are functions of the quantity $T\sqrt{K_2}/K_1$.

III. SIMULATION DETAILS

Many temperatures and densities have been studied, some of them coinciding with those from previous works [8,4,9] in order to obtain a general expression for the density and temperature dependence of the Mori and self-diffusion coefficients. We focus here on the self-diffusion coefficient as, being a single particle property, it can be obtained with

TABLE I. Self-diffusion coefficients, in units of $\sigma(\epsilon/m)^{1/2}$, obtained from the mean-square displacements and from exponential, Gaussian, hyperbolic secant, and Joslin-Gray closures. In the fourth column and in parentheses the results are taken from Refs. [8,4], respectively. The standard errors are $\approx \pm 5\%$ for the simulation self-diffusion coefficients and one digit in the last place for the Mori theory predictions. In the last row we give $\mathcal{S}$, the sum of the square of the differences between the MSD and Mori prediction for the self-diffusion coefficients.

t^*	ρ^*	D_{MSD}	$D_{\mathrm{Ref.\,[8]}}$	$D_{\exp}$	D_G	D_{sech}	D_{JG}
0.71	0.8000	0.045	0.041	0.071	0.057	0.045	0.058
0.75	0.8442	0.031		0.065	0.052	0.041	0.054
(0.722)	0.8442	(0.030)		(0.063)	(0.050)	(0.040)	(0.052)
1.00	0.7200	0.091	0.10	0.122	0.097	0.077	0.091
(1.05)	(0.731)	(0.097)		(0.125)	(0.099)	(0.079)	(0.092)
0.86	0.7608	0.066	0.066	0.098	0.078	0.062	0.075
1.20	0.4774	0.30	0.31	0.288	0.230	0.184	0.177
1.22	0.6470	0.14	0.16	0.180	0.144	0.115	0.125
1.81	0.600	0.26	0.28	0.301	0.24	0.191	0.192
1.81	0.700	0.20	0.17	0.226	0.18	0.144	0.157
1.90	0.801	0.13	0.13	0.201	0.16	0.128	0.146
1.90	0.801	(0.13)		(0.175)	(0.139)	(0.111)	(0.128)
2.57	0.200	1.45	1.54	1.67	1.33	1.06	0.73
2.51	0.300	1.00	0.89	1.05	0.84	0.67	0.52
2.47	0.400	0.68	0.611	0.73	0.58	0.46	0.39
2.48	0.500	0.45	0.478	0.54	0.43	0.34	0.32
(2.50)	0.500	(0.471)		(0.532)	(0.425)	(0.339)	(0.306)
2.50	0.600	0.34	0.38	0.39	0.31	0.25	0.25
2.50	0.803	0.18	0.18	0.23	0.18	0.14	0.16
2.50	(0.800)	(0.173)		(0.220)	(0.176)	(0.140)	(0.157)
2.51	1.040	0.07	0.07	0.13	0.10	0.08	0.10
(2.50)	(1.0648)	(0.051)		(0.110)	(0.088)	(0.070)	(0.092)
3.46	0.400	0.79		0.98	0.78	0.62	0.52
		(0.819)		(0.971)	(0.774)	(0.618)	(0.500)
3.46	0.500	0.65	0.66	0.68	0.54	0.43	0.39
3.41	0.600	0.44	0.43	0.50	0.40	0.32	0.31
3.46	0.700	0.36		0.39	0.31	0.25	0.26
		(0.331)		(0.382)	(0.305)	(0.243)	(0.249)
3.54	0.803	0.25	0.20	0.30	0.24	0.19	0.21
3.35	1.040	0.10	0.10	0.16	0.13	0.10	0.13
4.45	0.700	0.44	0.46	0.50	0.40	0.32	0.32
4.45	0.803	0.30	0.31	0.38	0.30	0.24	0.26
$\Sigma_{i=1}^{24}(D_{i,\mathrm{MSD}}$	$-$	$D_{i,\mathrm{closure}})^2$	$=$	0.141	0.079	0.479	0.840

greater precision than any of the other transport coefficients. The technical procedure we have followed here is similar to that we developed previously for the mass and size dependence of a solute particle in a solvent system at a given (T^*,ρ^*) state point [13,14].

A Lennard-Jones (LJ) interaction potential, $U(r)=4\epsilon[(\sigma/r)^{12}-(\sigma/r)^6]$ was used, where ϵ is the well depth and σ is the diameter of the particle taken as the units of the energy and length, respectively. The interaction was truncated at an intermolecular separation of $r=2.5\sigma$, and the spherical distance for the Verlet neighbor table was $r=2.75\sigma$ [15]. The Tøxvaerd algorithm was used with a time step of $h=0.005(m\sigma^2/\epsilon)^{1/2}$ [16]. The algorithm permits the direct calculation of K_1 and K_2 during the simulation as being a function of the force [Eq. (5)] and its first time derivative [Eq. (6)]. The updated canonical ensemble (NVT) in the Nosé-Hoover formulation [18,19] was used with an isothermal relaxation time of $\tau_T=0.05$ [17,20]. The time average for the mean-squared displacement in Eq. (1) was taken over 500 time steps and the simulations were carried out for $2-5\times10^5$ time steps. Cubic periodic boundary conditions were used on systems containing $N=256$ particles as in Refs. [8,4], where it was shown that there is a negligible system size dependence of the transport coefficient for N values equal to or larger than $N=256$ [21]. The simulated systems included high-density metastable states exemplified by the state point $(T^*,\rho^*)=(0.71,1.04)$, up to high temperature and low-density fluid states typified by $(T^*,\rho^*)=(4.45,0.2)$.

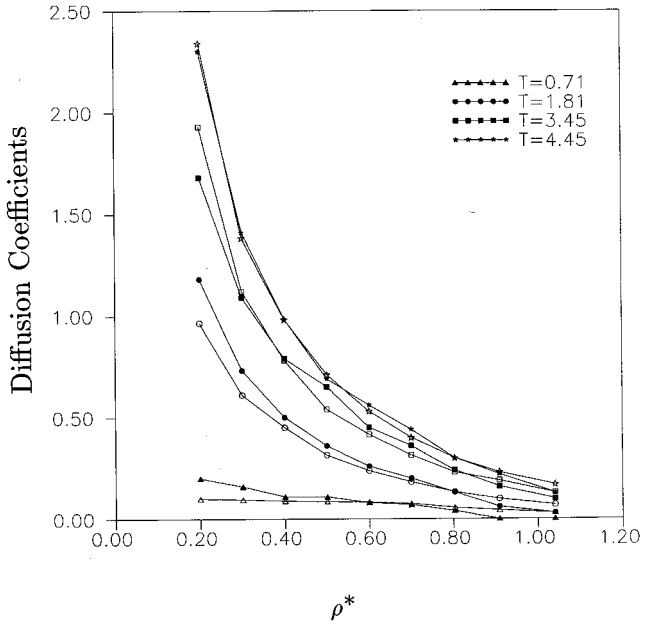

FIG. 1. Density dependence of the diffusion coefficients for several of the isotherms of Table I. The filled in symbols are the results using the MSD method, while open symbols correspond to those calculated from the Gaussian approximation closure.

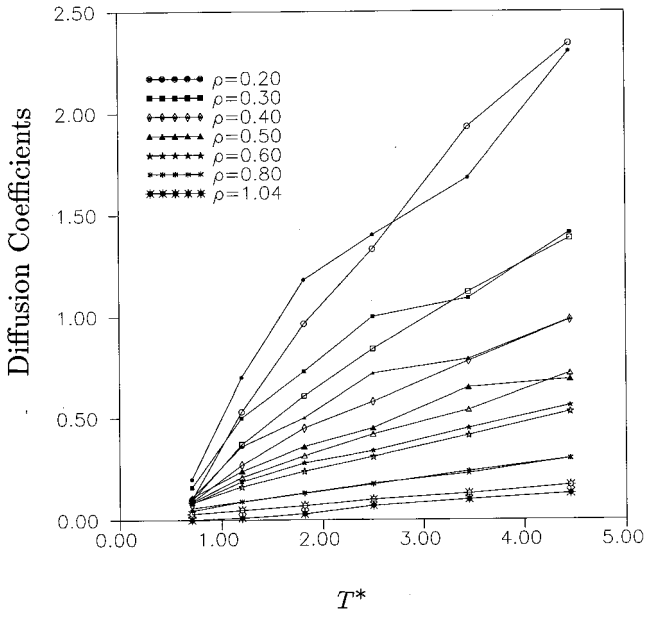

FIG. 2. The temperature dependence of the self-diffusion coefficients for a series of isochores.

IV. RESULTS

The Mori series and MSD self-diffusion coefficients are given in Table I for a wide range of (T^*,ρ^*). The diffusion coefficients obtained directly from the simulation using the MSD method are in good agreement with previous calculations (e.g., [8,4]) showing the expected general trend that D increases with temperature and decreases with increasing density. If we now compare the several closures, we see first that the self-diffusion coefficients obtained with the exponential approximation are larger than those obtained by the MSD method, except for $T^*=1.20$ and $\rho^*=0.4774$. This difference for a given value of T^* increases with the density, but for a given density tends to decrease with increasing T^*. Considering all the cases studied, we find that typically D_{exp} is about 25% greater than D_{MSD}.

The secant hyperbolic closure gives smaller values for the diffusion coefficient than the MSD method for most of the cases studied. However, the differences get smaller with increasing density for a given temperature and become equal (and even $D_{\text{sech}}>D_{\text{MSD}}$) for the lower temperatures and higher densities; see, for example, the data entries for $(T^*,\rho^*)=(0.71,0.8)$ and $(0.75,0.8442)$ in Table I.

A comparison between the Joslin-Gray closure and the MSD method shows a clear crossover behavior. At a given temperature, $D_{\text{MSD}}>D_{\text{JG}}$ for the low densities where there can be a large difference (of up to $\sim$100%) between the two calculated values. This difference not only diminishes with the increasing density, but the relation reverses for mid-to-high densities. A good example of this trend can be seen in Table I for $T^*\simeq 2.5$. The Gaussian approximation is similar to the JG method in its relationship with the MSD method. However there are significant quantitative differences. The Gaussian and Joslin-Gray closures are quite similar in the first four state points in the table but for $T^*\geqslant 1.20$ we find $D_G>D_{\text{JG}}$, with the D_G consequently much closer to D_{MSD}. The crossover of the D_G values from below to above the D_{MSD} values, which we find also for JG occurs at lower densities. There are smaller relative differences between D_{MSD} and D_G, as can be confirmed from Table I and as also seen in Fig. 1 for the $T^*=1.81$ isotherm.

In order to come to a conclusion about the best closure for the diffusion coefficient the standard deviation in the differences for the 24 evenly distributed state points studied have been calculated. These are shown in the last row of Table I. The Gaussian approximation has the smallest standard deviation of the four closures. We propose that the Gaussian closure is, on balance, the best representation of the MSD re-

TABLE II. Parameters characterizing the linear dependence of the self-diffusion coefficient with temperature for the densities in which the linear regression can be applied (see Fig. 2). The simulation derived data have been fitted to the analytic form, $D(T^*)=a+bT^*$. The upper row corresponds to the coefficients obtained from the MSD calculations and the lower row to those obtained from the Gaussian approximation. In the last column, $\mathcal{S}$ represents the sum of the squares of the differences between the MSD and Mori prediction for the self-diffusion coefficients, as in the last row in Table I.

ρ^*	a	b	$10^4\mathcal{S}$
0.60	0.030	0.122	24
	0.017	0.116	4
0.70	0.012	0.099	5
	0.021	0.086	1
0.80	0.005	0.067	1.2
	0.015	0.064	0.7
0.91	−0.030	0.057	7.8
	0.013	0.050	0.7
1.04	−0.030	0.037	1.6
	0.004	0.037	0.2

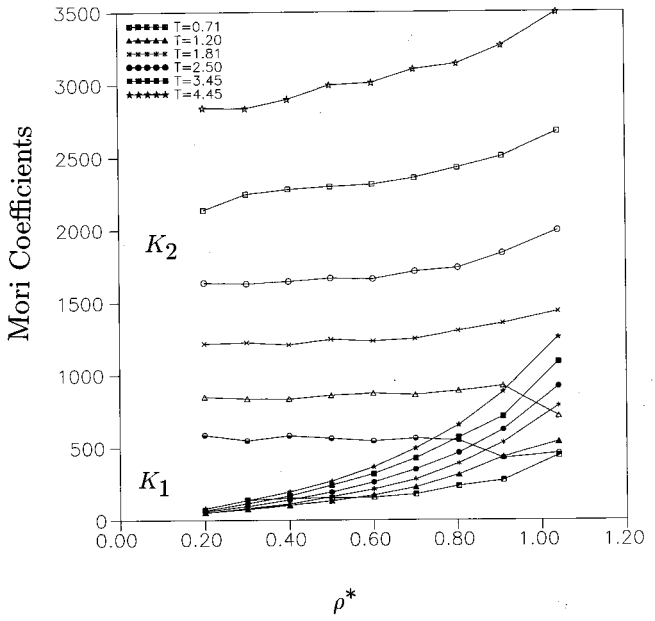

FIG. 3. Density dependence of the Mori coefficients for all the isotherms studied. Filled in (open) symbols correspond to the first (second) Mori coefficient, directly obtained from the (NVT) simulation.

sults, with the JG method the worst of the four closure schemes. The Gaussian gives best overall agreement with the MSD results, particularly for mid-to-high temperatures and for any density. In the following discussion we will concentrate on the (T^*,ρ^*) dependence of the self-diffusion coefficient obtained by the Gaussian approximation with the first two Mori coefficients.

Although we have chosen six temperatures ($T^*=0.71$, 1.20, 1.81, 2.50, 3.45, and 4.45), and nine densities ($\rho^*=0.20$, 0.30, 0.40, 0.50, 0.60, 0.70, 0.80, 0.91, and 1.04) at which to perform our study, not all of the data have been

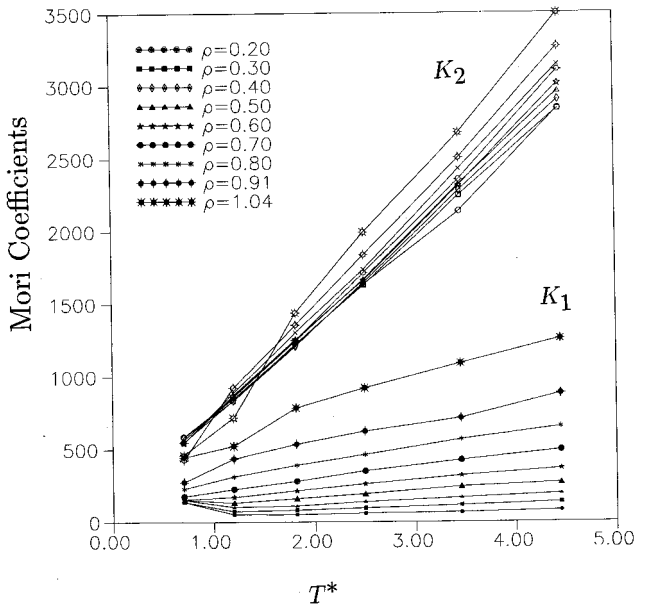

FIG. 4. As for Fig. 3, except the temperature dependence of the Mori coefficients for a series of isochores is shown.

TABLE III. The coefficients specifying the linear dependence of the first Mori coefficient on temperature for all the densities studied. The simulation data have been fitted to the analytic form $K_1(T^*)=c+dT^*$. The asterisk (dagger) means that the lowest (two lowest) temperatures have been taken out for the linear regression. The last column is as for Table II.

ρ^*	c	d	$10^{-2}\mathcal{S}$
0.20*	38.77	8.78	0.36
0.30*	49.53	19.36	0.15
0.40*	64.57	29.46	0.65
0.50*	83.86	43.50	1.57
0.60	110.66	58.70	1.87
0.70	125.42	85.32	3.22
0.80	173.20	111.98	11.80
0.91*	284.60	131.94	10.60
1.04†	468.83	178.54	1.45

plotted in the following figures to avoid too many overlapping lines. In Fig. 1, the diffusion coefficients obtained directly by molecular dynamics D_{MSD} shown as filled-in symbols and D_G by open symbols are plotted for several isotherms. The decay of the diffusion coefficient is similar for both methods; however, there are notable relative trends. For the low-to-middle range temperatures (up to $T^*\sim 2.50$) and densities (up to $\rho^*\sim 0.7$) the self-diffusion coefficients by MSD are larger than those calculated from the Gaussian approximation. However, for $\rho^*\approx 0.8$ we find that $D_G \approx D_{\mathrm{MSD}}$ at all temperatures. For higher densities, in contrast, $D_G > D_{\mathrm{MSD}}$ for the low-to-mid temperatures but tend to be approximately equal for the higher temperatures. This trend is also apparent in Fig. 2, which compares the self-diffusion coefficients along a series of isochores. The statistical fluctuations in the D_{MSD}, obtained are much greater than those from the Gaussian approximation, for the low-to-mid densities (up to $\rho^*\approx 0.5$). At higher density the two sets of self-diffusion coefficients show a near-linear dependence on temperature with quite good agreement between D_G and D_{MSD}; in fact, they coincide for $\rho^*=0.8$ at all temperatures considered. For completeness, the coefficients of the linear

TABLE IV. The parameters characterizing the linear dependence of the second Mori coefficient on temperature for all the densities studied. The experimental data have been fitted to $K_2(T^*)=e+fT^*$. The asterisk (dagger) means that the lowest (two lowest) temperatures have been taken out for the linear regression. The last column is as for Table II.

ρ^*	e	f	$10^{-3}\mathcal{S}$
0.20	140.17	596.65	6.57
0.30	105.18	615.40	0.72
0.40	97.70	627.91	3.74
0.50	88.85	643.15	1.78
0.60	69.58	654.60	3.62
0.70	37.56	680.50	4.55
0.80	46.25	691.32	1.94
0.91*	50.01	718.19	1.21
1.04†	33.3	775.05	1.67

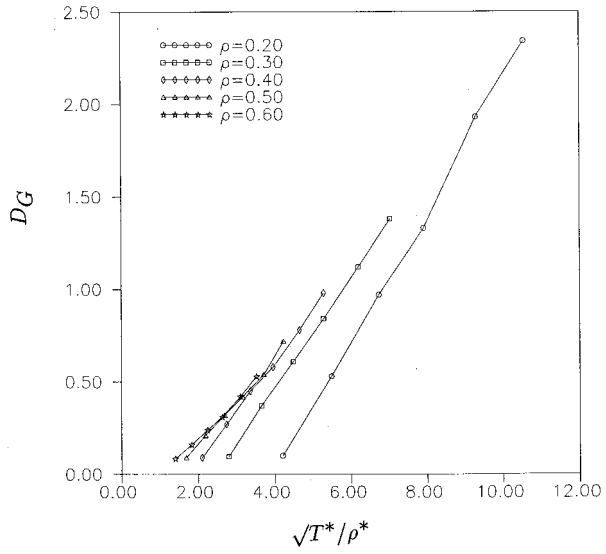

FIG. 5. $\sqrt{T^*}/\rho^*$ dependence of the Gaussian self-diffusion coefficient for low-to-mid densities.

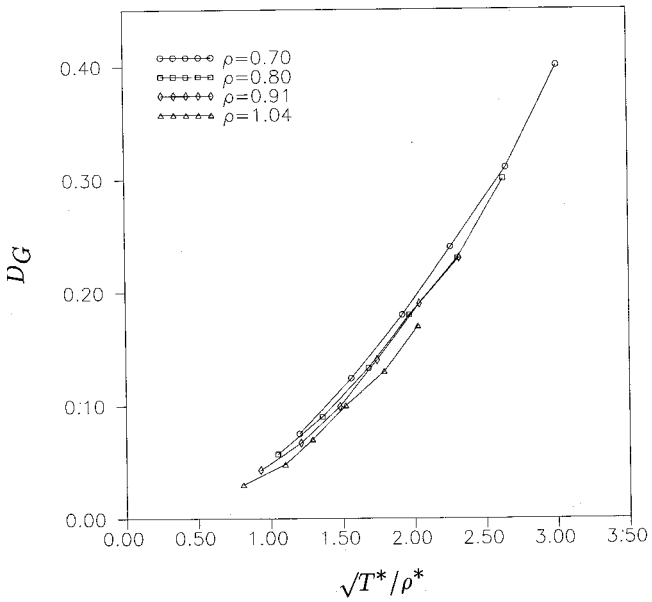

FIG. 6. The same as Fig. 5 for mid-to-high densities.

regression for the diffusion coefficient obtained by MSD and Gaussian approximation are listed in Table II for the densities where temperature linearity can be applied.

Turning now to the (T^*,ρ^*) dependence of the Mori coefficients, Fig. 3 gives the density dependence of the first two Mori coefficients (K_1, filled-in symbols; K_2 open symbols) along several isotherms. The K_2 values are typically several orders of magnitude greater than the corresponding K_1. Both coefficients increase with temperature and density, varying less dramatically with density for K_2 than for K_1. When the temperature decreases the K_2 coefficient becomes essentially density independent, especially for $T^*=0.71$ and 1.20. At the higher densities for these low-temperature isotherms, the Mori coefficients show anomalous behavior that we attribute to the fact that the fluids are in the two-phase region of the LJ phase diagram [4]; there is a sharp decay in K_1 and K_2, as can be seen in Fig. 3 for $(T^*,\rho^*)=(0.7,0.91)$, (0.7,1.04), and (1.2,1.04). The Mori coefficients are essentially linear with temperature at fixed density (see Fig. 4) apart from the several low-temperature high-density metastable points. The K_1 straight line regimes shift upwards with isochore density; the slope and ordinate intercept increase. The corresponding K_2 straight lines appear to pivot about a point in the plane with increasing slopes and decreasing ordinate intercept. This ''point of gyration'' is close to the lowest temperature considered, i.e., $T^*=0.71$, which can be considered to be the minimum temperature for which linear regression can be applied since below that value the system is metastable [4]. In Tables III and IV the coefficients obtained from the linear regression for $K_1(T^*)$ and $K_2(T^*)$ have been collected. The K_1 values shown in Figs. 3 and 4 are in good agreement with those reported in Ref. [9] for the same state points.

Experimentally the self-diffusion coefficient in dense fluids goes as $\sim T^*/\rho^*$ at constant pressure [22,23]. This is in contrast to the gas limit $\sqrt{T^*}/\rho^*$ at zero density. The linear temperature dependence arises from the synergistic effect of increased kinetic energy and liquid expansion with increasing temperature (the latter makes available additional free volume in which the molecules can move). Along isochores this second contribution is not present and we recover the gas temperature dependence at all densities, as observed many times by MD simulation for simple fluids (e.g., [24,25]). In Fig. 5 we have plotted D_G vs $\sqrt{T^*}/\rho^*$ for several isochores. There is linear behavior for D_G for low-to-mid densities (especially for $\rho^*=0.3$) at all temperatures studied, and the parameters of the linear regression of these data are presented in Table V. The near-linear regions of the two lowest density isochores are practically parallel. However, for higher densities the slopes tend to diminish with

TABLE V. The coefficients specifying the linear dependence of the Gaussian Mori theory prediction for the self-diffusion coefficient on temperature for the low-to-mid densities studied. The simulation data have been fitted to the analytic form $D_G(T^*)=g+h(\sqrt{T^*}/\rho^*)$. Last column is as in Table II.

ρ^*	g	h	$10^3\mathcal{S}$
0.20	−1.42	0.36	7.0
0.30	−0.74	0.30	0.2
0.40	−0.49	0.28	0.9
0.50	−0.32	0.24	2.0
0.60	−0.22	0.21	0.8

TABLE VI. The coefficients specifying the dependence of the Gaussian self-diffusion coefficient on temperature for the mid-to-high densities studied. The simulation data have been fitted to the analytic form $D_G(T^*)=i+j(\sqrt{T^*}/\rho^*)+k(\sqrt{T^*}/\rho^*)^2$. Last column is as in Table II.

ρ^*	i	j	k	$10^5\mathcal{S}$
0.70	−0.019	0.040	0.032	6
0.80	−0.008	0.026	0.034	5
0.91	−0.021	0.038	0.031	7
1.04	0.001	0.001	0.040	3

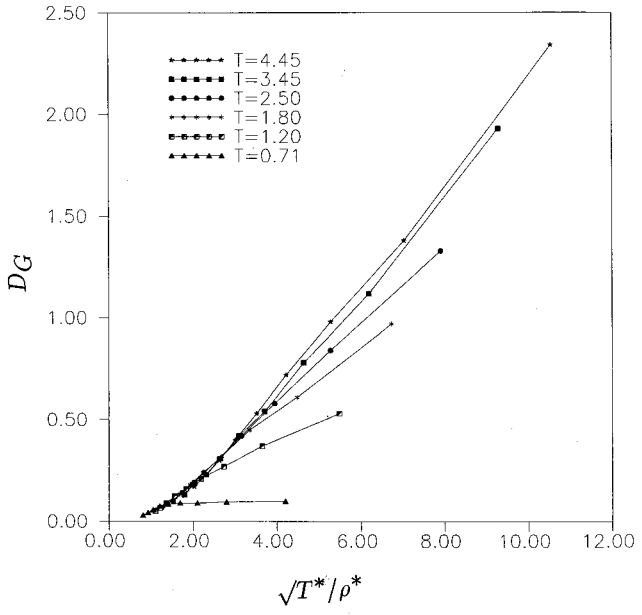

FIG. 7. $\sqrt{T^*}/\rho^*$ dependence of the Gaussian self-diffusion coefficient for all the isotherms studied.

increasing density. For mid-to-high densities ($0.7 \leqslant \rho^* \leqslant 1.04$) a linear regression, it is no longer the best fit to the data, as can be seen also in Fig. 6. In fact, a second-order polynomial regression in powers of $\sqrt{T^*}/\rho^*$ is required (see Table VI, which lists the coefficients of these regressions). Note that for the highest density, the D_G values are practically proportional to $(\sqrt{T^*}/\rho^*)^2$, as noted by Levesque and Verlet, for similar densities [6]. Figure 7 and Table VII give the D_G vs $\sqrt{T^*}/\rho^*$ for all the isotherms. As can be seen, all the isotherms are close to being straight lines with significant overlap at the high densities and low temperatures (seen in the bottom left part of Fig. 7). Taking the best fit as the reference line ($T^*=2.5$ in Table VII) one can see that in the high-temperature limit (e.g., $T^*=3.45$ and 4.45) the straight lines practically coincide while for the lower temperatures their slopes decrease drastically and curve over tending to zero slope for the lowest temperature of $T^*=0.71$ (excluding the metastable state points in this).

V. DISCUSSION AND CONCLUSIONS

As suggested in our previous work [26] we have evaluated the first two Mori coefficients and self-diffusion coefficient for many (T^*,ρ^*) values to determine the state point dependence of these coefficients, a similar procedure to that which we used for the effects of mass and volume changes of a single solute particle [13,14]. Table I reveals, in agreement with Ref. [4], that the relative merits of the closures depend on the point in the LJ phase diagram at which the simulation is performed. The hyperbolic secant closure is closest to the MSD values, for temperatures and densities close to the triple point, e.g., $(T^*,\rho^*)=(0.71,0.80)$ and $(T^*,\rho^*)=(0.75,0.8442)$. The Joslin-Gray or even the exponential closure are better for higher temperatures and lower densities [see, for example, the states $(T^*,\rho^*)=(1.0,0.72)$ and $(T^*,\rho^*)=(1.20,0.4774)$ in Table I]. The best overall behavior for a wide spectrum of temperature and densities is for the Gaussian approximation. It could be argued that the superiority of the Gaussian closure arises merely from a cancellation of errors, but of all the *ad hoc* closures it is the only one that leads to a time-reversible velocity autocorrelation function, and therefore its success may have more fundamental significance. The Gaussian function representation of the self-diffusion coefficient in terms of the two Mori coefficients, Eq. (12), has advantages over the direct method as the slope of the mean-square displacements can have large uncertainty, especially at lower densities and moderate temperatures, as can be seen in Fig. 2. In fact, the Gaussian approximation (or some improvement thereof) could ultimately provide a better route to the self-diffusion coefficient than by the direct method, especially for the lower temperatures and densities (see Fig. 2) where molecular dynamics is not an efficient technique for exploring phase space. However, for mid-to-high densities, both methods are consistent in giving the same linear behavior with temperature, as is shown in Fig. 2, and from their corresponding linear regression parameters given in Table II.

TABLE VII. The coefficients specifying the dependence of the Gaussian self-diffusion coefficient over all the isotherms studied. The simulation data have been fitted to the analytic form $D_G(\rho^*)=l+m(\sqrt{T^*}/\rho^*)$. Last column is as in Table II.

T^*	l	m	$10^3\mathcal{S}$
4.45	−0.36	0.25	3
3.45	−0.32	0.24	4
2.50	−0.20	0.19	4
1.80	−0.14	0.17	10
1.20	−0.05	0.11	3

The self-diffusion coefficients are linear with density for the lowest isotherm considered, but decay as a higher-order polynomial for the higher temperature isotherms; the order of the polynomial increases with temperature (see Fig. 1). For the isotherm $T^*=1.20$ a second-order dependence on density is found, whereas for $T^*=1.81$ and 2.50 it is third order and for $T^*=3.45$ and 4.45 it is fourth order. This is the case for both the MSD and Gaussian approximation methods, the results from the latter being a better fit to a polynomial analytic form. The first Mori coefficient increases as a polynomial with density (see Fig. 3), from first order for the lowest isotherm $T^*=0.71$, to second order for the higher at $T^*=4.45$. In contrast, the second Mori coefficient is less density dependent, especially for the two lowest isotherms (at least for the state points in which the system remains an equilibrium liquid) and smoothly curves upwards with increasing density for the higher temperature isotherms. Both Mori coefficients are essentially linear with temperature at fixed density, with a slope increasing with density as can be seen in Fig. 4. In Tables III and IV the Mori coefficients are fitted to a linear regression in T^*.

As shown in Fig. 5 and Table V for low-to-mid densities the self-diffusion coefficients in the Gaussian approximation are linear in $(\sqrt{T^*}/\rho^*)$, as has been found in previous MD simulation studies [8,24,25]. Although for the higher densi-

ties a second-order polynomial in $\sqrt{T^*}/\rho^*$ is a better representation of the data (see Fig. 6 and Table VI). As D_G is proportional to $T\sqrt{K_2}/K_1$ from Eqs. (11) and (12), then we can conclude that $\sqrt{K_2}/K_1$ is proportional to $(\sqrt{T^*}\rho^*)^{-1}$.

Perhaps the most significant result from this work is the decreasing density and increasing temperature dependence of the second Mori coefficient when compared with the first Mori coefficient, which agrees with the conclusions made by Lee and Chung from their extensive study of the LJ system [7]. Lee and Chung found that the K_3 and higher-order Mori coefficients are weakly density dependent but increasingly temperature dependent, which could have implications for improved Mori series closures.

ACKNOWLEDGMENTS

The authors thank the British Council and Delegación de Investigación y Ciencia for supporting this work under the Collaboration Project (Acciones Integradas) between the U.K. and Spain. This work has also been supported in part by the Spanish DGICYT, Project No. PB95-0254. The computations were carried on a CONVEX 210 at the University of Extremadura's Computer Center.

[1] B. J. Berne and G. D. Harp, Adv. Chem. Phys. **17**, 63 (1970).
[2] H. Mori, Prog. Theor. Phys. **33**, 423 (1965); **34**, 399 (1965).
[3] S. Toxvaerd, J. Chem. Phys. **81**, 5131 (1984).
[4] D. M. Heyes and J. G. Powles, Mol. Phys. **71**, 781 (1990).
[5] D. M. Heyes, J. G. Powles, and Gil Montero, Mol. Phys. **78**, 229 (1993).
[6] D. Levesque and L. Verlet, Phys. Rev. A **2**, 2514 (1970).
[7] L. L. Lee and T.-H. Chung, J. Chem. Phys. **77**, 4650 (1982).
[8] D. M. Heyes, J. Chem. Soc. Faraday Trans. 2 **79**, 1741 (1983).
[9] K. Tankeshwar, J. Phys. Condens. Matter **7**, 9715 (1995).
[10] M. P. Allen and D. J. Tildesley, *Computer Simulation of Liquids* (Clarendon, Oxford, 1987).
[11] L. L. Lee, Physica A **100**, 205 (1980).
[12] C. G. Joslin and C. G. Gray, Mol. Phys. **58**, 789 (1986).
[13] J. J. Morales and M. J. Nuevo, J. Comput. Chem. **13**, 1119 (1992).
[14] M. J. Nuevo and J. J. Morales, Phys. Lett. A **178**, 114 (1993).
[15] L. Verlet, Phys. Rev. **159**, 98 (1967).
[16] S. Tøxvaerd, J. Comput. Phys. **47**, 444 (1982).
[17] S. Tøxvaerd, Mol. Phys. **72**, 159 (1991).
[18] S. Nosé, Mol. Phys. **52**, 255 (1984).
[19] W. G. Hoover, Phys. Rev. A **31**, 1695 (1985).
[20] L. F. Rull, J. J. Morales, and S. Toxvaerd, Phys. Rev. A **38**, 4309 (1988).
[21] D. M. Heyes, Phys. Rev. B **37**, 5677 (1988).
[22] J. L. Hildebrand, *Viscosity and Diffusivity: A Predictive Treatment* (Wiley, New York, 1987).
[23] J. J. van Loef, Physica B **103**, 133 (1981).
[24] J. P. J. Michels and N. J. Trappeniers, Physica A **116**, 516 (1982).
[25] M. Bishop and J. P. J. Michels, Chem. Phys. Lett. **94**, 209 (1983).
[26] M. J. Nuevo, J. J. Morales, and D. M. Heyes, Phys. Rev. E **51**, 2026 (1995).